Appl. Phys. A 79, 117–124 (2004)
DOI: 10.1007/s00339-003-2492-y

Applied Physics A
Materials Science & Processing

T. NATSUKI
K. TANTRAKARN
M. ENDO✉

Effects of carbon nanotube structures on mechanical properties

Faculty of Engineering, Shinshu University, Wakasato 4-17-1, Nagano-shi, 380-8553, Japan

Received: 30 September 2003/Accepted: 9 December 2003
Published online: 27 February 2004 •

ABSTRACT This paper describes a structural mechanics approach to modelling the mechanical properties of carbon nanotubes (CNTs). Based on a model of truss structures linked by inter-atomic potentials, a closed-form elastic solution is obtained to predict the mechanical properties of single-walled carbon nanotubes (SWNTs). Moreover, the elastic modulus of multi-walled carbon nanotubes (MWNTs) is also predicted for a group of the above mentioned SWNTs with uniform interval spacing. Following the structural mechanics approach, the elastic modulus, Poisson's ratio, and the deformation behaviors of SWNTs were investigated as a function of the nanotube size and structure. Poisson's ratio of SWNTs shows a chirality dependence, while the elastic modulus is insensitive to the chirality. The disposition of the strain energy of bonds shows quite a difference between the zigzag and armchair tubes subjected to axial loading. A zigzag tube is predicted to have a lower elongation property than an armchair tube.

PACS 62.20-x; 62.20.Dc; 62.25+g

1 Introduction

Carbon nanotubes (CNTs) have attracted growing interest due to their exceptional mechanical, thermal, and electrical properties [1–6]. One potential application of CNTs is in the development of CNT-based composites since the inclusion of CNTs within various matrices can obviously improve their physical properties. Qian et al. [7] have reported that the addition of just 1 wt. % CNTs to polystyrene results in an increases of elastic modulus and strength by approximately 35%–42% and 25%, respectively. In general, an accurate assessment of the properties of individual CNTs is essential for the development of CNT-based reinforced composites. Hence, the mechanical properties of CNTs have been the subject of a number of experimental [8–12] and theoretical studies [13–29, 31–33] since their discovery in 1991.

Experiment methods for measuring the mechanical properties of CNTs are mainly based on the techniques of transmission electron microscopy (TEM) and atomic force microscopy (AFM). Treacy et al. [8] have been the first to perform an experimental measurement of the elastic modulus in multi-walled carbon nanotubes (MWNTs). They have obtained a value of 1.8 ± 0.9 TPa by measuring thermal vibration using TEM. Later, a slightly lower value of 1.28 ± 0.59 TPa with little dependence of nanotube diameter was obtained by Wong et al. [9] using the AFM tip to bend anchored MWNTs. Yu et al. [10] have measured the tensile strength and modulus of MWNTs to be in the range from 11 to 63 GPa and 0.27 to 0.95 TPa, respectively. Krishnan et al. [11] have reported a study on single-walled carbon nanotubes (SWNTs) using the TEM technique. The SWNTs had a diameter range of 1.0–1.5 nm, and the elastic modulus was measured to be the mean value of $1.25–0.35/+0.45$ TPa. Yu et al. [12] have also obtained the mechanical responses of SWNT bundles under tensile loading. The values of elastic modulus ranged from 0.32 to 1.47 TPa with a mean value of 1.02 TPa, and a tensile strength from 13 to 53 GPa. These experiments have contributed to confirming that CNTs have exceptional mechanical properties. However, the experimental error bars are too large to state the characteristics of CNTs of different sizes and structures.

Computational simulation for predicting mechanical properties of CNTs has been regarded as a powerful tool relative to the experimental difficulty. The classical molecular dynamics (MD) and ab initio methods [13–21] have been used quite extensively. Yakobson and co-workers [13–16] have used the MD method for simulating the elasticity and plasticity properties, mechanism of strain release, and instabilities beyond a linear response. They have used a many-body interatomic potential with a continuum shell model and predicted an elastic modulus of about 5.5 TPa [13]. Hernandez et al. [17, 18] have predicted the elastic modulus and Poisson's ratio of SWNTs with different chiral vectors. Using a tight-binding method, they have reported a surface modulus of 0.42 TPa − nm. In general, ab initio methods gives more accurate results than MD simulation. Lier et al. [19] have obtained an elastic modulus of higher than 1 TPa by using the ab initio method. Lu [20, 21] has investigated the elastic properties of nanotubes and nanoropes using an empirical force-constant model. He has reported that Young's modulus and the shear modulus are less than 1.0 and 0.45 TPa, respectively. Odegard et al. [22] have proposed modelling the CNT as a continuum by equating the potential energy with that of the representative volume element (RVE). They have also applied RVE methods

✉ Fax: +81-26/269-5208, E-mail: endo@endomoribu.shinshu-u.ac.jp

to the constitutive model of CNT composite systems [23]. Ruoff and Lorents [24] have suggested the use of the elastic modulus of graphite by neglecting the change in the atomic structure when a piece of graphene sheet is rolled into a nanotube. For the mechanical properties of MWNTs, however, the theoretical work is relatively sparse [25, 26]. Tu et al. [26] have revealed the effective elastic modulus of MWNTs to be dependent on their layer number and to have a large varying range.

Molecular and solid mechanics have been highly developed to describe material properties with micro- and macro-structures, respectively. However, an available computational power is demanded for the MD method. A well established continuum mechanics model on a nanoscale is a challenging task for computational simulation. In this paper, we present a closed-form expression for modelling the elastic moduli of both SWNTs and MWNTs based on a truss structure model. The effects of tube curvature on the mechanical properties of SWNTs are considered in the closed-form solution. The elastic properties of CNTs, including the elastic modulus, Poisson's ratio, and the strain energy are discussed as a function of nanotube size and structure.

2 The structure of carbon nanotubes

A SWNT is formed by folding a single graphene sheet to form a hollow tube composed of carbon hexagons. The fundamental carbon nanotube is classified into three categories in terms of their helicity [27]: zigzag, armchair, and chiral. The atomic structure of carbon nanotubes can be indexed by a pair of integers (n, m), corresponding to a lattice vector $\boldsymbol{C}_h = n\boldsymbol{a}_1 + m\boldsymbol{a}_2$ on the graphite plane, where $\boldsymbol{a}_1$ and $\boldsymbol{a}_2$ are unit vectors of the two-dimensional graphene sheet. The symmetry groups of carbon nanotubes are denoted by zigzag $(m = 0)$ and armchair $(n = m)$ tubes. The integers (n, m) uniquely determine the size of the SWNT. The radius, ϱ_n, of nanotubes can be determined by using the rolling graphene sheer model:

$$\varrho_n = \frac{\sqrt{3}b}{2\pi}\sqrt{\left(n^2+m^2+mn\right)}, \tag{1}$$

where b is the carbon–carbon bond length.

Considering the effective wall thickness of SWNT, t, the effective radius, ϱ_{na}, is defined as

$$\varrho_{na} = \frac{\sqrt{3}b}{2\pi}\sqrt{\left(n^2+m^2+mn\right)} + \frac{t}{2}. \tag{2}$$

For a MWNT, the number of layers, N, and the effective cross-sectional area, A_{eff}, can be given as

$$N = 1 + \frac{(\varrho_o - \varrho_i)}{h},$$
$$A_{eff} = 2\pi t\left\{N\varrho_i + \sum_{i=1}^{N}(i-1)h\right\}, \tag{3}$$

where h is the distance between layers of the MWNT. ϱ_i and ϱ_o are the innermost and outermost radii, respectively.

3 Theoretical approach

3.1 *Molecular potential energy*

The mechanical properties of solid materials must ultimately depend on the strength of their interaction bonds. The bonded and non-bonded interactions of the atoms in a molecular structure can be described by using molecular mechanics. The forces that exist for each bond are described by the force field so that these forces contribute to the total molecular potential energy of a molecular system. In general, the total potential energy of the force field can be expressed as the sum of bonding and nonbonding energies:

$$E^m = \sum E^{\varrho} + \sum E^{\theta} + \sum E^{\tau} + \sum E^{nb} \tag{4}$$

where E^{ϱ} , E^{θ}, and E^{τ} , are the bonding energy associated with bond stretching, angle variation, and torsion, respectively. E^{nb} is the nonbonding energy that consists of van der Waals forces and electrostatic interaction (see Fig. 1).

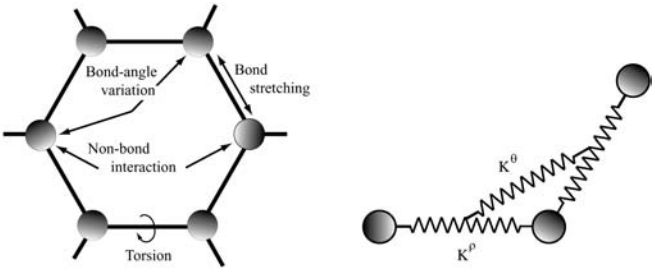

FIGURE 1 Molecular mechanics and frame structure model

In small strain conditions, harmonic energy functions are generally used when the bond length of molecular systems is near its equilibrium position. For the CNTs subjected to axial loading, torsion and weakly nonbonding interactions can be regarded as negligible. Therefore, the system potential energy of the nanotube with carbon-to-carbon bonds can be simplified as [22]

$$E^m = \frac{1}{2}\sum_i K_i^{\varrho}(\Delta b_i)^2 + \frac{1}{2}\sum_i K_i^{\theta}(\Delta\theta_j)^2, \tag{5}$$

where Δb_i is the elongation of bond i , and $\Delta\theta_j$ is the variance of bond angle j. K_i^{ϱ} and K_i^{θ} are the force constants associated with the bond stretching and bending, respectively.

For the truss structure as shown in Fig. 1 (right), K^{ϱ} can be used for modelling the axial deformation of the carbon-to-carbon bond, and K^{θ} for the angular distortion between the bonds. The stretching and bending bonds are strongly coupled. In the molecular force field of nano-structured materials subjected to lower load, the stretching and bending forces can be given as

$$F = K^{\varrho}\Delta b,$$
$$M = K^{\theta}\Delta\theta. \tag{6}$$

3.2 *Elastic properties for SWNTs*

Figure 2 shows the schematic illustration of the (5, 5) armchair tube subjected to axial tension. The molecular

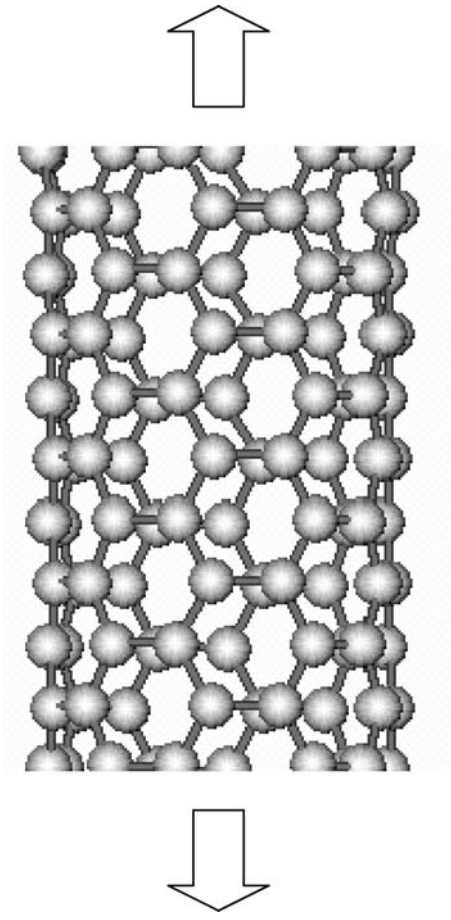

FIGURE 2 Schematic illustration of the (5, 5) armchair tube subjected to axial tensile

mechanics model is substituted with a frame structure so as to form an equivalent-continuum body with the truss structures. Figure 3 shows the three-dimensional schematic illustration of the force and moment acting on a bond, and the geometrical relationship among the atoms. Ω is the plane perpendicular to the axes of the nanotube, and $n-n'$ is a line of intersection between the Ω plane and BAC plane. In CNTs with small curvature, the atoms of the hexagonal lattice are no longer confined to a plane when the graphene sheet is rolled. The angle γ, related to the curvature effect, is equal to $\pi/2n$ (Fig. 3).

We now consider the force and moment exerted on a bond. The stretch and angular deformations of the bond are caused by the axial force and bending moment, respectively. For an armchair tube subjected to the tension stress, σ_a, the force and the moment acting on the AB bond can be given by

$$Q = \sigma_a tb(1+\cos\theta),$$
$$M = M_A + M_B = Qb\cos\theta. \tag{7}$$

According to the elastic relations given by (6), we obtain the equilibrium equations about the bond extension and angle variation, given by

$$Q\sin\theta = K^{\varrho}\delta^{\varrho}_{AB},$$
$$M_j = K^{\theta}(2\Delta\theta) + K^{\theta}|\Delta\alpha|\cos\varphi,$$
$$j = A, B, \tag{8}$$

where δ^{ϱ}_{AB} are the extension of the A–B bond. φ is the torsion angle between planes containing C–A–B and B–A–D bonds. Each bond connects with four other bonds and associates with four bond angles. $2\Delta\theta$ and $\Delta\alpha$ in (8) are the two angle variations between the A–B bond and its adjacent bonds connected with atom A (or atom B). According to the geometrical relation shown in Fig. 3 (right), we obtain

$$\cos(\pi-\alpha) = \cos\theta\cos\gamma,$$
$$\cos\varphi = \frac{\mathrm{tg}\theta}{\mathrm{tg}(\pi-\alpha)}. \tag{9}$$

Differentiating both sides of the first part of (9), we obtain the relation between the neighbor bond angle variances as

$$\Delta\alpha = -\frac{\sin\theta\cos\gamma}{\sin(\pi-\alpha)}\Delta\theta. \tag{10}$$

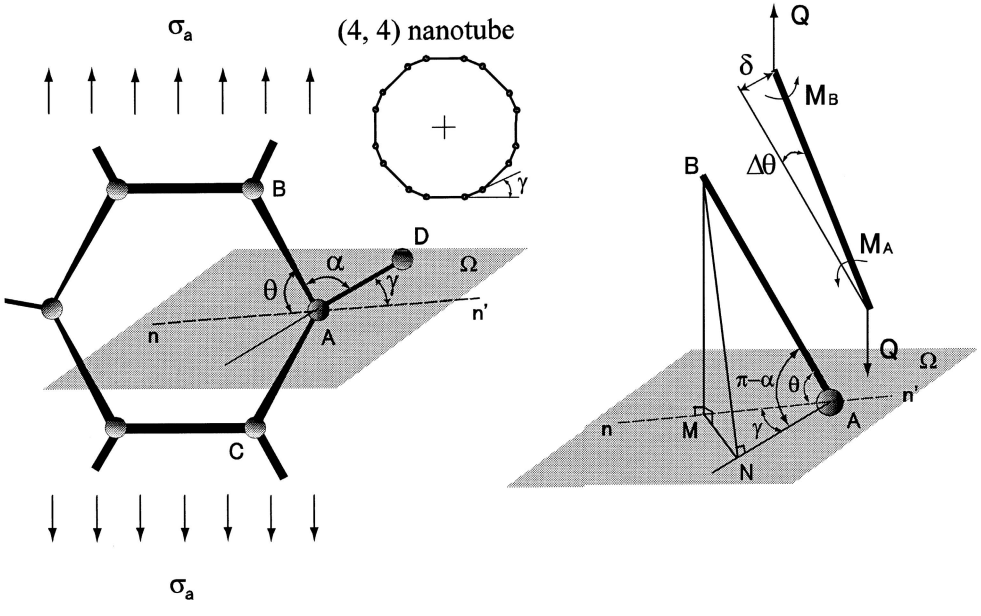

FIGURE 3 Analysis of forces and geometrical relations for an armchair tube

The axial strain (ε_a) and the hoop strain (ε_h) of the armchair tube can be given as

$$\varepsilon_a = \frac{\delta\cos\theta + \delta_{AB}^{\varrho}\sin\theta}{b\sin\theta},$$
$$\varepsilon_h = \frac{\delta_{AB}^{\varrho}\cos\theta - \delta\sin\theta}{b(1+\cos\theta)}. \tag{11}$$

For an SWNT with an effective radius of, ϱ_{na}, the elastic modulus of an armchair tube is defined as

$$E_a = \frac{2\varrho_n t}{\varrho_{na}^2}\left(\frac{\sigma_a}{\varepsilon_a}\right). \tag{12}$$

Substituting (7)–(11) into (12), we obtain the elastic modulus of an armchair tube:

$$E_a = \frac{2\varrho_n}{\varrho_{na}^2}\left(\frac{\sin\theta}{1+\cos\theta}\right)\frac{\lambda_a K^{\theta} K^{\varrho}}{b^2 K^{\varrho}\cos^2\theta + \lambda_a K^{\theta}\sin^2\theta}, \tag{13}$$

where

$$\lambda_a = 4 + \frac{2\sin^2\theta}{\sin\alpha\cos\theta}\frac{\cos\gamma}{tg(\pi-\alpha)} \tag{14}$$

Poisson's ratio of the armchair tube can be defined as the ratio between the circumferential and the axial strains, so we have

$$\nu_a = -\frac{\varepsilon_h}{\varepsilon_a} = \frac{(b^2K^{\varrho} - \lambda_a K^{\theta})\sin^2\theta\cos\theta}{(b^2K^{\varrho}\cos^2\theta + \lambda_a K^{\theta}\sin^2\theta)(1+\cos\theta)}. \tag{15}$$

The angle θ is regard as an almost unchanged constant when a planar graphene sheet is rolled into a nanotube. Putting $\theta = \pi/3$ into eqns. (13), (14) and (15), gives the simplified elastic modulus and Poisson's ratio as follows:

$$E_a = \frac{\lambda_a K^{\theta} K^{\varrho}}{3b^2K^{\varrho} + 9\lambda_a K^{\theta}}\left(\frac{8\sqrt{3}\varrho_n}{\varrho_{na}^2}\right),$$
$$\nu_a = \frac{b^2K^{\varrho} - \lambda_a K^{\theta}}{b^2K^{\varrho} + 3\lambda_a K^{\theta}}, \tag{16}$$

where

$$\lambda_a = \frac{16 + 2\cos^2\gamma}{4 - \cos^2\gamma} \tag{17}$$

The variations of the bond length and angle with axial strain are given by

$$\delta_{AB}^{\varrho} = \frac{3b\lambda_a K^{\theta}\varepsilon_a}{b^2K^{\varrho} + 3\lambda_a K^{\theta}}, \tag{18}$$

$$\Delta\theta = \frac{\sqrt{3}b^2K^{\varrho}\varepsilon_a}{b^2K^{\varrho} + 3\lambda_a K^{\theta}},$$
$$\Delta\alpha = \frac{\sqrt{3}\cos\gamma}{\sqrt{4-\cos^2\gamma}}\Delta\theta. \tag{19}$$

The following theoretical approach for a zigzag tube is similar to that for the armchair tube. According to the geometrical relation of the armchair tube shown in Fig. 4, we get

$$\sin\frac{\alpha}{2} = \sin\theta\cos\left(\frac{\pi}{2n}\right),$$
$$\mathrm{tg}\frac{\alpha}{2} = \cos\varphi\,\mathrm{tg}\theta. \tag{20}$$

When a SWNT is subjected to an applied stress, σ_z, the force and the moment are given as

$$P = \sigma_z t b\sin\theta,$$
$$M = M_A + M_B = Pb\sin\theta. \tag{21}$$

The equilibrium equations are

$$P\cos\theta = K^{\varrho}\delta_{AB}^{\varrho},$$
$$2P = K^{\varrho}\delta_{AB}^{\varrho}, \tag{22}$$

$$M_j = K^{\theta}\Delta\theta + K^{\theta}|\Delta\alpha|\cos\varphi,$$
$$j = \mathrm{A,B}. \tag{23}$$

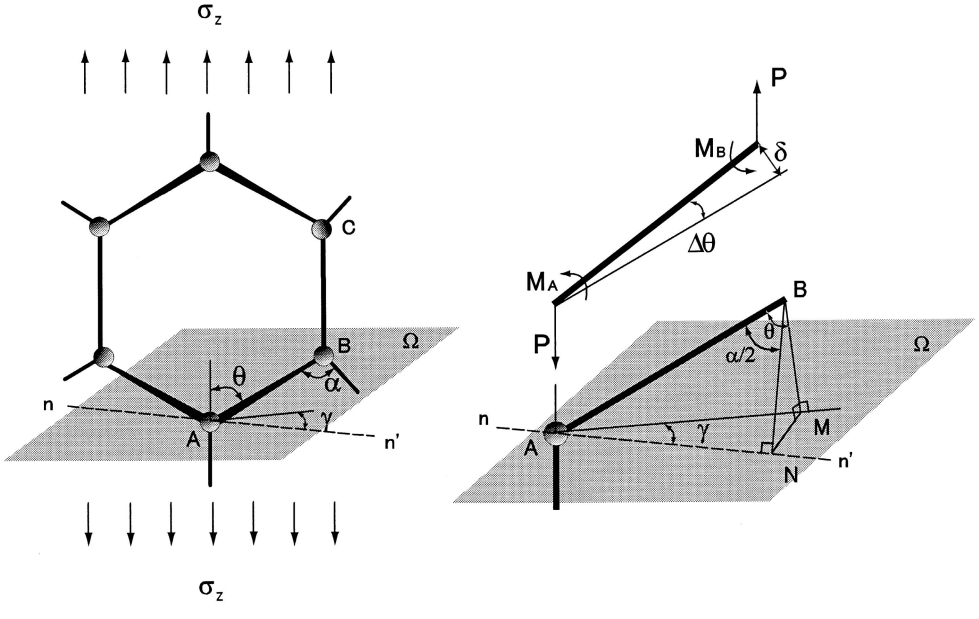

FIGURE 4 Analysis of forces and geometrical relations for a zigzag tube

The axial and hoop strains of the zigzag tube are given respectively as

$$\varepsilon_z = \frac{\delta \sin\theta + \delta^{\varrho}_{AB}\cos\theta + \delta^{\varrho}_{BC}}{b(1+\cos\theta)},$$
$$\varepsilon_h = \frac{\delta^{\varrho}_{AB}\sin\theta - \delta\cos\theta}{b\sin\theta} \tag{24}$$

Putting $\theta = \pi/3$, we obtain the elastic modulus and Poisson's ratio of a zigzag tube, given as follows:

$$E_z = \frac{\lambda_z K^{\theta} K^{\varrho}}{3b^2 K^{\varrho} + 9\lambda_z K^{\theta}} \left(\frac{8\sqrt{3}\varrho_n}{\varrho_{na}^2}\right),$$
$$\nu_a = \frac{b^2 K^{\varrho} - \lambda_z K^{\theta}}{b^2 K^{\varrho} + 3\lambda_z K^{\theta}}, \tag{25}$$

where

$$\lambda_z = \frac{8 - 2\cos^2\gamma}{4 - 3\cos^2\gamma} \tag{26}$$

The variation of the bond length and angle are given by

$$\delta^{\varrho}_{AB} = \frac{3b\lambda_z K^{\theta}\varepsilon_z}{b^2 K^{\varrho} + 3\lambda_z K^{\theta}},$$
$$\delta^{\varrho}_{BC} = \delta^{\varrho}_{AB} \tag{27}$$

$$\Delta\theta = \frac{\sqrt{3}b^2 K^{\varrho}\varepsilon_z}{b^2 K^{\varrho} + 3\lambda_z K^{\theta}},$$
$$\Delta\alpha = \frac{2\cos\gamma}{\sqrt{4 - 3\sin^2\gamma}}\Delta\theta. \tag{28}$$

Substitution of (18),(19), (27), and (28) into (5) can yield the variation of the strain energy of CNTs with axial strain.

According to the condition of the continuum body, the rotational shear modulus is easily given as

$$G = \frac{\varrho_{na}^4 - (\varrho_{na} - t)^4}{t\varrho_{na}^4}\left(\frac{\sqrt{3}}{3}\,\frac{\lambda_i K^{\theta} K^{\varrho}}{b^2 K^{\varrho} + \lambda_i K^{\theta}}\right), \tag{29}$$

where the parameter λ_i $(i = a, b)$ is taken by λ_a for an armchair tube, and λ_z for a zigzag tube.

3.3 *Elastic properties for MCNTs*

MWNTs can be considered as a group of co-axial SWNTs packed together with a uniform interval layer [5, 26]. We assume that all co-axial tubes of shells have the same axial strain after loading on the two ends. The interactions between the neighboring tubes can be neglected since van der Waals force is considered to be relatively weak. Therefore, each individual tube has a structural feature with a monolayer of atoms. Based on classical elastic theory, the elastic modulus can be estimated by the effective radius and cross-sectional area of MWNTs. We yield the elastic modulus for the MWNTs with an ignorable curvature effect:

$$E_m = \frac{A_{\text{eff}}}{\pi t\left[(\varrho_0 + t/2)^2 - (\varrho_i - t/2)^2\right]}\,\frac{8\sqrt{3}K^{\theta}K^{\varrho}}{b^2 K^{\varrho} + 18K^{\theta}} \tag{30}$$

After substituting (3) into the above equation, the elastic modulus of the MWNT as a function of the number of layers, N, is given by

$$E_m = \frac{8\sqrt{3}N}{[(N-1)h+1]}\,\frac{K^{\theta}K^{\varrho}}{b^2 K^{\varrho} + 18K^{\theta}}, \quad 1 < N \le 1 + 2\varrho_o/h. \tag{31}$$

4 Results and discussions

In this computational simulation, the two main types of carbon nanotubes, namely, the armchair and zigzag tubes were discussed. The initial carbon–carbon bond length was taken as 0.142 nm [27]. The predicted values of the elastic properties were affected largely by the assumption of the wall thickness of CNTs [28–30]. The assumptions of different wall thickness, such as 0.066 nm [13], 0.69, and 0.57 nm [22], have been reported in other publications. It should be pointed out that the concept of the wall thickness of SWNTs does not make any true sense since it is only given as a continuum assumption. The wall thickness of SWNTs composed of atomic structures should be regarded as quite thin. In the present simulation, the effective wall thickness of the SWNTs' layers can be assumed to be zero. In the force field of CNTs, the force constants of the stretching and bending were taken as those of the graphene sheet [31]

$$K^{\varrho}/2 = 46\,900\ \text{kcal/mole/nm}^2,$$
$$K^{\theta}/2 = 63\ \text{kcal/mole/rad}^2. \tag{32}$$

The force constants of the graphene sheet will change slightly in a rolled sheet. The simulation was valid only for the CNTs whose radii are not very small since the model neglects the effects of curvature on the force constants.

4.1 *Elastic modulus*

Comparing (16) and (17) with (25) and (26), we find that the expressions for predicting an armchair tube have the same forms as those for a zigzag tube except for the difference in λ_a and λ_z. Based on the closed expressions, Fig. 5 shows the variation of elastic modulus of SWNTs with diameter. Both axial and shear moduli increase rapidly with a decrease in nanotube diameter. For smaller tubes, the elastic modulus of the armchair tube is slightly larger than that of the zigzag tube. As the tube diameter increases, the elastic modulus of the armchair and zigzag tubes begin to have the same value. This result has been also obtained and discussed by an earlier MD simulation [2, 32]. A SWNT's diameter is usually in the range of 1.0–1.5 nm [11]. Based on the present theory, we calculate the axial modulus of the SWNTs to be 1.1–0.73 TPa, and the shear modulus to be 0.86–0.55 TPa. The maximum elastic modulus is estimated to be about 2.2 TPa in the thinnest SWNT with a 0.43 nm diameter. Figure 6 shows the comparison of the present theory with the MD simulation. It can be seen that the predicted values obtained from the nanoscale continuum model agree well with those reported in the literature [28, 29].

MWNT's diameters are usually in the range of 5.0–50 nm. The distance between layers of the MWNTs is 0.34 nm [1, 3].

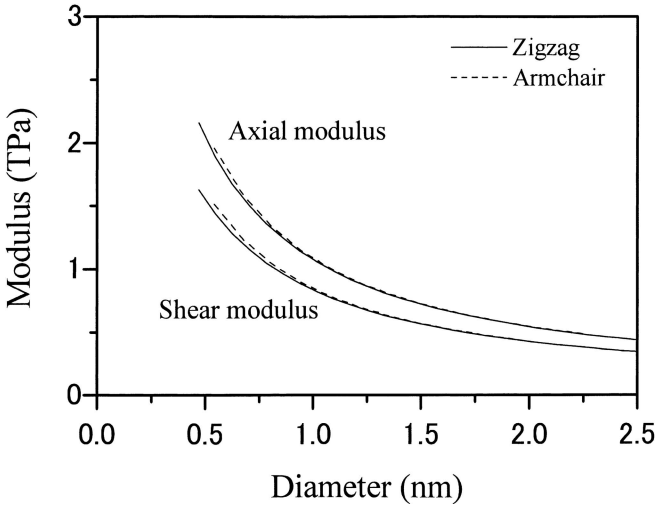

FIGURE 5 Variation of elastic modulus with nanotube diameter for the armchair and zigzag tubes

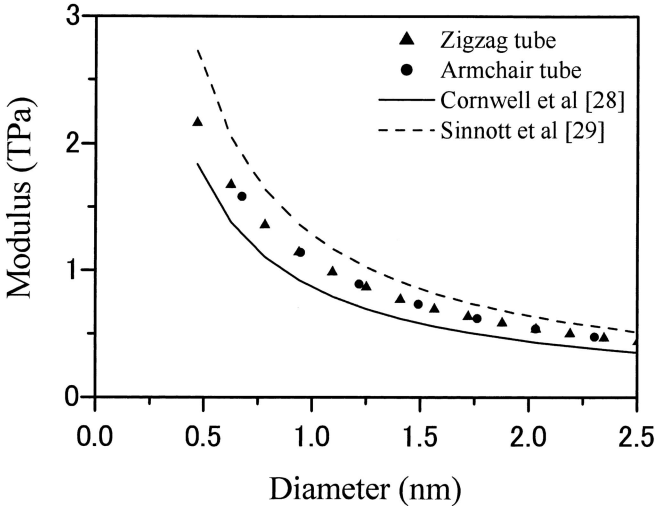

FIGURE 6 Comparison of the present theory with the existing MD simulations

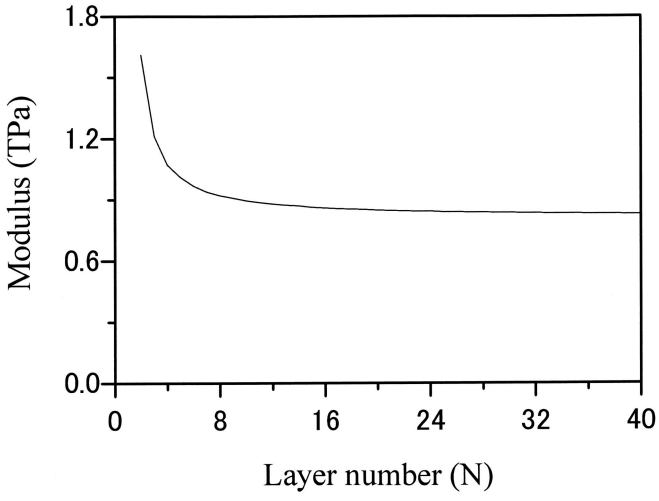

FIGURE 7 Variation of modulus with the layer number of WMCNTs

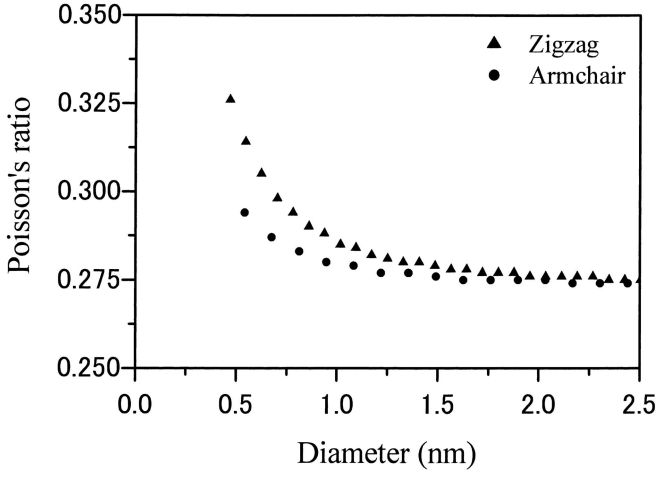

FIGURE 8 Variation of Poisson's ratio with nanotube diameter for the armchair and zigzag tubes

According to equation (31), the elastic modulus of MWNTs is independence of the tube diameter. Figure 7 shows the variation of the elastic modulus of MWNTs with layer number. It can be found that the elastic modulus of the MWNTs is dependent on the number of shells and has a varying range of 1.6 to 0.8 TPa. However, the elastic modulus becomes insensitive to the layer number when $N \geq 8$. Tu et al. [26] have reported that the elastic modulus of MWNTs varied from 1.7 to 1.05 TPa up to infinity for the double-walled nanotube.

4.2 *Poisson's ratio*

Figure 8 shows Poisson's ratio as a function of the tube diameter for the armchair and zigzag tubes. Poisson's ratio of the zigzag tube exhibits more sensitivity to the diameter than that of the armchair tube. As the diameter of the SWNTs increases, Poisson's ratio approaches a steady value of 0.27, corresponding to that of the flat graphence, calculated by minimizing the strain energy [20, 21]. SWNTs are predicted to have a Poisson's ratio ranging from 0.27 to 0.33.

4.3 *Strain energy*

Based on the molecular potential energy given by (5), the strain energy of armchair and zigzag tubes as a function of the axial strain is shown in Fig. 9. The calculated strain energy within elastic limits shows reasonably agreement with that obtained from classical MD simulations [28, 33]. The (10, 10) armchair and (17, 0) zigzag tubes have a nearly equal diameter of 1.33 nm. It is found that the strain energy of SWNTs is independent of the chirality but depends slightly on the tube diameter. Comparing with the (17, 0) nanotube, the (8, 0) nanotube shows a slightly lower variation of strain energy with axial strain. For narrow diameter nanotubes, the carbon-to-carbon bonds can be weakened by the high curvature of the surface of the nanotubes.

Figures 10 and 11 show the strain energy of the bond stretching and bending for the (10, 10) armchair and (17, 0) zigzag tubes, respectively. According to the calculation, the dispositions of the strain energy are quite different in the zigzag and armchair tubes although their total strain energy is almost the same. The strain energy subjected to axial loading is mainly that of the bond stretching in atom structures. The strain energy of the B−C bonds aligned along the axis of

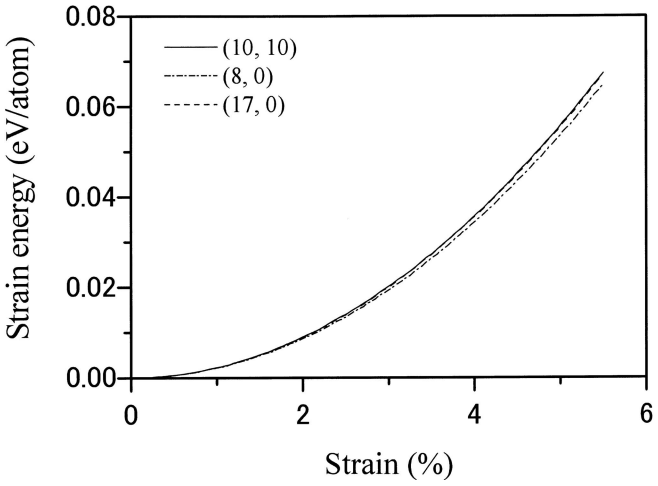

FIGURE 9 Strain energy per atom for nanotubes as a function of the axial strain

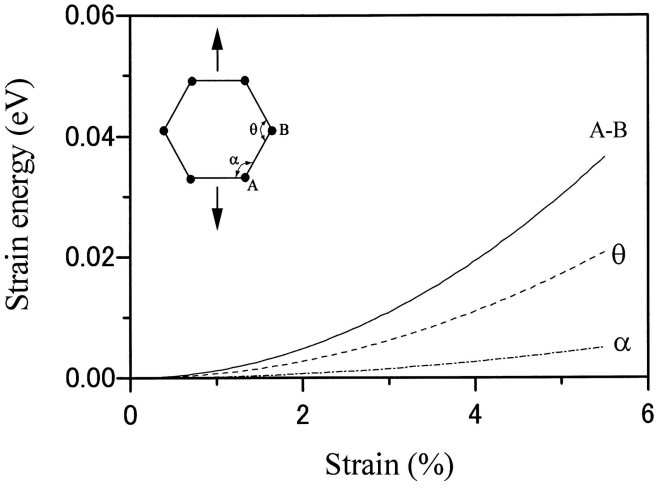

FIGURE 10 Dispersion of the strain energy of bond stretching and bending in an armchair tube

zigzag tubes is much higher than other bonds and bond angles. From the atom deformation mechanics, the failure mode of chemical bonds depends mainly on their bond elongation. Due to the elongation of the B−C bond, the fracture of the zigzag tube occurs at a lower strain when compared with the armchair tube. The armchair tube has higher elongation and strength properties than the zigzag tube.

5 Conclusions

Based on a link between molecular and solid mechanics, we present a simple approach to predicting the elastic properties of CNTs. The closed-form elastic solution is able to serve as a good approximation for the mechanical properties. The elastic modulus, Poisson's ratio, and strain energy are investigated as a function of the nanotube size and structure. According to the present model, we calculate the elastic modulus to be 1.1–0.73 TPa for SWNTs, and 1.6–0.8 TPa for MWNTs. Poisson's ratio is predicted to be 0.27–0.33, which shows the chirality dependence. Compared with the armchair tube, the fracture of the zigzag tube is predicted to occur at a lower strain since the bonds parallel to the axis of the

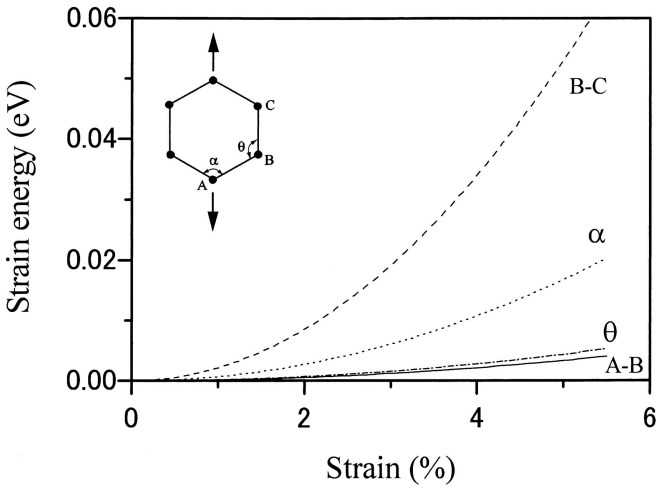

FIGURE 11 Dispersion of the strain energy of bond stretching and bending in a zigzag tube

tubes are easily subjected to larger strain energy under tensile loading.

ACKNOWLEDGEMENTS This work was supported by the CLUSTER of the Ministry of Education, Culture, Sports, Science, and Technology of Japan.

REFERENCES

1 K.T. Lau, D. Hui: Composites: Part B **33**, 263 (2002)
2 B.I. Yakobson, P.H. Avour, in: *Carbon nanotubes*, Chapt. 9, ed. by M.S. Dresselhaus, P.H. Avouris, (Springer Verlag, Berlin-Heidelberg 2001) p. 287
3 E.T. Thostenson, Z. Ren, T.W. Chou: Comp. Sci. Tech. **61**, 1899 (2001)
4 L. Vaccarini, C. Goze, L. Henrard, E. Hernandez, P. Bernier, A. Rubio: Carbon **38**, 1681 (2000)
5 J.P. Salvetat, J.M. Bonard, N.H. Thomson, A.J. Kulik, L. Forro, W. Benoit, L. Zuppiroli: Appl. Phys. A **69**, 255 (1999)
6 L.S. Schadler, S.C. Giannaris, P.M. Ajayan: Appl. Phys. Lett. **73**, 3842 (1998)
7 D. Qian, E.C. Dickey, R. Andrews, T. Rantell: Appl. Phys. Lett. **76**, 2868 (2000)
8 M.M.J. Treacy, T.W. Ebbesen, J.M. Gibson: Nature **381**, 678 (1996)
9 E.W. Wong, P.E. Sheehan, C.M. Lieber: Sci. **277**, 1971 (1997)
10 M.F. Yu, O. Lourie, M.J. Dyer, K. Moloni, T.F. Kelly, R.S. Ruoff: Sci. **287**, 637 (2000)
11 A. Krishnan, E. Dujardin, T.W. Ebbesen, P.N. Yianilos, M.M.J. Treacy: Phys. Rev. B **58**, 14013 (1998)
12 M.F. Yu, B.S. Files, S. Arepalli, R.S. Ruoff: Phys. Rev. Lett. **84**, 5552 (2000)
13 B.I. Yakobson, C.J. Brabec, J. Bernholc: Phys. Rev. Lett. **76**, 2511 (1996)
14 B.I. Yakobson: Appl. Phys. Lett. **72**, 918 (1998)
15 M.B. Nardelli, B.I. Yakobson, J. Bernholc: Phys. Rev. B **57**, R4277 (1998)
16 K.N. Kudin, G.E. Scuseria, B.I. Yakobson: Phys. Rev. B **64**, 235406 (2001)
17 E. Hernandez, C. Goze, P. Bernier, A. Rubio: Phys. Rev. Lett. **80**, 4502 (1998)
18 E. Hernandez, C. Goze, P. Bernier, A. Rubio: Appl. Phys. A. **68**, 287 (1999)
19 G.V. Lier, C.V. Alsenoy, V.V. Doren, P. Geerlings: Chem. Phys. Lett. **326**, 181 (2000)
20 J.P. Lu: J. Phys. Chem. Solids. **58**, 1649 (1997)
21 J.P. Lu: Phys. Rev. Lett. **79**, 1297 (1997)
22 G.M. Odegard, T.S. Gates, L.M. Nicholson, K.E. Wise: NASA Langley Res. Center, NASA-2002-TM211454
23 G.M. Odegard, V.M. Harik, K.E. Wise, T.S. Gates: NASA Langley Res. Center, NASA-2001-TM211044

24 R.S. Ruoff, D.C. Lorents: Carbon **33**, 925 (1995)
25 S. Govindjee, J.L. Sackman: Solid State Commun. **110**, 227 (1999)
26 Z.H. Tu, Z.C. Ou-Yang: Phys. Rev. B **65**, 233 407 (2002)
27 M.S. Dresselhaus, G. Dresselhaus, R. Saito: Carbon **33**, 883 (1995)
28 C.F. Cornwell, L.T. Wille: Solid State Commun. **101**, 555 (1997)
29 S.B. Sinnott, O.A. Shenderova, C.T. White, D.W. Brenner: Carbon **36**, 1 (1998)
30 T. Vodenitcharova, L.C. Zhang: Phys. Rev. B **68**, 165 401 (2003)
31 W.D. Cornell, P. Cieplak, C.I. Bayly, I.R. Gould, K.M. Merz, D.M. Ferguson, D.C. Spellmeyer, T. Fox, J.W. Caldwell, P.A. Kollman: J. Am. Chem. Soc. **117**, 5179 (1995)
32 V.N. Popov, V.E. Van Doren, M. Balkanski: Phys. Rev. B **61**, 3078 (2000)
33 D. Srivastava, M. Menon, K. Cho: Phys. Rev. Lett. **83**, 2973 (1999)